Summer 6-13-2017

Characterizing the Viscoelastic Behavior of PDMS/PDPS Copolymers

Mark E. Small

Mark Small

Candidate

Mechanical Engineering

Department

This thesis is approved, and it is acceptable in quality and form for publication:

Approved by the Thesis Committee:

Dr.Yu-lin Shen , Chairperson

Dr.Walter Gerstle

Dr.Ryan Jamison

Characterizing the Viscoelastic Behavior of PDMS/PDPS Copolymers

by

Mark E. Small

B.S., Mechanical Engineering, University of New Mexico, 2015

THESIS

Submitted in Partial Fulfillment of the
Requirements for the Degree of

Master of Science
Mechanical Engineering

The University of New Mexico

Albuquerque, New Mexico

July, 2017

Dedication

To my brothers in arms, and all of those that have paid the ultimate sacrifice. I would not be where I am now without the prices you have paid.

"The most important six inches on the battlefield is between your ears"
– Gen. James "Mad Dog" Mattis

Acknowledgments

I would like to thank my advisors, Professor Yu-Lin Shen, and Professor Walter Gerstle. I would also like to thank my mentors, Ryan Jamison, and Kurtis Ford for their help and support.

Characterizing the Viscoelastic Behavior of PDMS/PDPS Copolymers

by

Mark E. Small

B.S., Mechanical Engineering, University of New Mexico, 2015

M.S., Mechanical Engineering, University of New Mexico, 2017

Abstract

Viscoelasticity is the property of materials that exhibits both viscous and elastic characteristics when undergoing deformation. In polymeric materials, the mechanical behavior is dominated by this viscoelastic phenomenon. Creating computational models for these materials can be quite complicated due to their frequency dependent and temperature dependent material properties. The research presented in this paper will use state of the art methods to fully develop a material model for a filled polydimethylsiloxane-polydiphenynlsiloxane (PDMS/PDPS) copolymer foam that has yet to be characterized. Mechanical properties of PDMS/PDPS copolymers are currently being studied to assess engineering performance, and to provide accurate models that can be used to gain a fundamental understanding of the material behavior. The properties for this material have been measured using multiple experiments. All of the parameters required to populate the Simplified Potential Energy Clock (SPEC) model were measured. The SPEC model can now be used to accurately predict the behavior of the material under different shock and loading environments.

Contents

Contents

List of Figures

List of Figures

List of Figures

List of Tables

Chapter 1

Introduction

This work focuses on a particular polymer, called PDMS/PDPS copolymer. It's favorable thermal and mechanical properties make it ideal for numerous engineering applications. The viscoelastic thermal and mechanical material properties for the PDMS/PDPS copolymer of interest have not been determined until now. The composition of the copolymer presented in this research is described in Section 1.1. To provide a foundation for how these materials behave during arbitrary strain conditions the basic concepts of linear viscoelasticity are presented in Sections 2.1-2.3. The material properties were determined by using various experiments. An overview of these experiments is provided in Section 1.2. Once the material properties were determined through experimentation, they were used to calibrate a material model. The calibration techniques used are presented in Sections 4.1-4.2. All of the properties required for the Simplified Potential Energy Clock (SPEC) model were determined. An accurate viscoelastic SPEC model for this material will enable more accurate predictive models. The SPEC model is explained in Section 2.4. Additional experiments and analysis were preformed to validate the calibrated SPEC model for the PDMS/PDPS copolymer. These experiments are presented in Section 3.1.4. The overall goal of this research was to accurately predict the viscoelastic behavior of the

PDMS/PDPS copolymer in preload and shock environments. Accurately predicting the behavior of the material during these environments will allow for better design and engineering for its applications. Some of the materials applications include gaskets, tires, and aircraft.

1.1 Material

One of the most commonly used silicone elastomers is poly(dimethyl siloxane) (PDMS). Recently, the use of copolymers between PDMS and poly(diphenyl siloxane)(PDPS) have garnered attention. The attention is justified due to some of the unique thermal and mechanical properties the PDMS/PDPS copolymer possess such as, their ability to withstand shock environments. The viscoelastic properties of the material can be used for design purposes in these environments.

The PDMS/PDPS copolymer is part of a polymer family known as silicone rubber. Silicone rubbers are elastomeric copolymers consisting of a silicone polymer that contains carbon, hydrogen, and oxygen. The siloxane polymer of interest consists of dimethyl (DMS), diphenyl (DPS), and methyl vinyl (MVS) siloxane monomer units. The composition is approximately 90.7 wt% DMS, 9.0 wt% DPS, between 0.1 and 0.5% MVS, and 6.8 wt% ethoxy-endblock siloxane processing aid.

1.2 Overview of Experiments

Several of the viscoelastic properties for PDMS/PDPS were obtained using dynamic mechanical analysis (DMA). One of the most commonly used instruments for conducting a DMA is the forced resonance analyzer. This apparatus, using a drive shaft, applies either an axial or a torsional sinusoidal force to a suspended specimen. The

frequency of the machine is varied to determine the viscoelastic characteristics. The DMA performed for PDMS/PDPS is presented in full detail in Section 3.1.1.

Another characterization technique that was used is thermal mechanical analysis (TMA). TMA was used to cool, heat, and calculate the resulting thermal strain of the material. The resulting thermal strain measurements were used to determine the materials thermal mechanical properties. The TMA preformed for the PDMS/PDPS copolymer is explained in Section 3.1.2.

The bulk modulus for the material was also measured. A pressure dilatometer was used to determine the volumetric response of the material. A sample of the material was suspended in a hydraulic fluid and then a hydrostatic pressure was applied. The bulk modulus can be calculated by the volumetric response. The pressure dilatometry experiment is explained in Section 3.1.3

To get a better understanding of the calibrated models behavior an oscillatory test was performed to obtain the uniaxial storage modulus. For this experiment the sample was clamped at both ends and an oscillatory strain was applied. This experiment is explained in Section 3.1.4.

Additionally, a three point bend test was performed to obtain the flexural storage modulus. A rectangular sample was simply supported at opposite ends while an oscillatory force was applied to the center of the sample. The three point bend test will be used to validate the calibrated viscoelastic model. This experiment is explained in section 3.1.4.

1.3 Material Model

Viscoelastic material models can be used in commercial Finite Element Analysis (FEA) software packages to determine the materials response to different loading environments. Software packages such as ANSYS, Abaqus, and Sierra use material models that include Neo-Hookian, Mooney-Rivlin, and SPEC. However, using these material models is nontrivial due to polymers complex relationship between stress and strain that is dependent on time. There are multiple approaches that can be used to overcome the obstacles with modeling viscoelastic materials. The methods used in this research is presented in Section 2.3.1.

Chapter 2

Viscoelastic Theory

2.1 Viscoelastic Behavior

Materials exhibit both viscous and elastic characteristics when undergoing deformation. This behavior is called "viscoelasticity." Viscoelastic behavior was first studied in the nineteenth century by eminent figures, such as Boltzmann, Coriolis, Gauss, and Maxwell [2]. The constitutive equations for linear viscoelasticity are based on some of the early mathematical modeling of relaxation and creep in silk, glass fibers, and rubber [3]. It was determined that the mechanical properties of viscoelastic materials depends upon time. Because of this dependence on time, the material exhibits multiple phenomena such as creep, stress relaxation, hysteresis, and strain-rate dependent stiffness. If the stress is held constant as seen in Figure 2.1a, the strain increases with time. This behavior is known as creep and it is illustrated in Figure 2.1b.

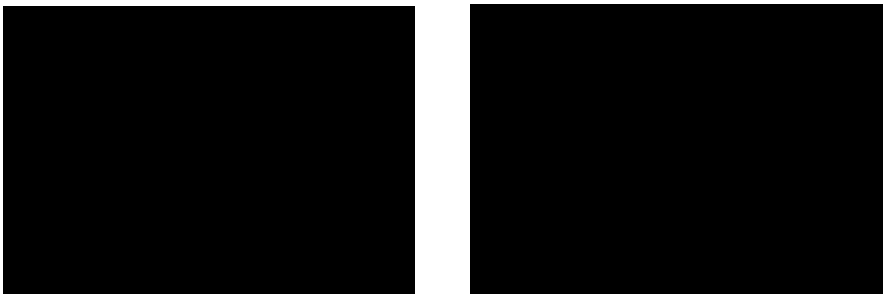

(a) Cause: Constant Stress (b) Effect: Increased Strain

Figure 2.1: Creep behavior. If a constant stress is applied to a viscoelastic material the resulting strain will increase.

However, if the strain is held constant as seen in Figure 2.2a, the stress decreases with time. This behavior is known as stress relaxation and is illustrated in Figure 2.2b.

(a) Cause: Constant Strain (b) Effect: Stress Relaxation

Figure 2.2: Stress relaxation behavior. If a constant strain is applied to a viscoelastic material the resulting stress will decrease over time.

Another phenomenon viscoelastic materials exhibit is the effects of hysteresis and strain-rate dependent stiffness that occur during loading and unloading. Hysteresis is the energy lost during cyclic loading, and it can be seen on the stress vs. strain plot in Figure 2.3.

Figure 2.3: Hysteresis effect. Viscoelastic material during loading and unloading.

It is also important to note that the stiffness of a viscoelastic material is dependent upon the rate at which it is being deformed [4]. This behavior is known as strain-rate dependence and is illustrated in Figure 2.4.

Figure 2.4: Strain-rate dependence of a viscoelastic material.

Arguably most materials exhibit some viscoelastic response [2]. Synthetic polymers display large viscoelastic effects. Depending on the application of the material these responses can be significant.The mathematical formulation of viscoelasticity theory is presented in this chapter with the aim of enabling prediction of the material response to an arbitrary loading history.

2.2 Linear Viscoelasticity

The siloxane polymer characterized in this research is assumed to be a linear viscoelastic material. A material model using linear viscoelasticity must satisfy two assumptions: first, the relationship between stress and strain is linear; second, the relaxation modulus is independent of the applied strain level [2]. The relationship between stress and strain are still time dependent. This means that the current mechanical state of the material depends on the previous loading history. To get a better understanding of this effect on the polymer, a fundamental background describing the transient behavior of viscoelastic materials has to be outlined.

2.2.1 Transient Behavior

The relationship between stress and strain within the linear elastic region of these solid materials can be described by Hooke's law, where stress, σ, is proportional to the strain, ϵ. Hooke's law can be expressed as:

$$\sigma = E\epsilon \tag{2.1}$$

where E is the Young's Modulus of the material. The use of Hooke's law to approximate the relationship between stress and strain is an excellent assumption for solid materials with infinitesimal strains within the linear elastic region. However, it is important to note that all materials deviate from Hooke's law in some way [2]. Viscoelastic materials are those for which the relationship between stress and strain is dependent on time. If the strain in Eq. 2.1 is applied instantaneously, it can be represented by ϵ_o. The time dependent stress response to an instantaneous strain

application is given by:

$$\sigma(t) = E(t)\epsilon_o \tag{2.2}$$

where $E(t)$ is known as the relaxation modulus, which is a material property that characterizes the stress relaxation over time. For viscoelastic materials, the stress will decrease with time if the instantaneous strain is held constant. In linear viscoelastic materials, $E(t)$ is independent of the strain level; that is, $E(t)$ is a function of time alone [4]. Stress relaxation can also be observed during shear and volumetric deformation, and the relaxation functions are represented by $G(t)$ and $K(t)$, respectively. A plot of the relaxation modulus vs. time is illustrated in Figure 2.5.

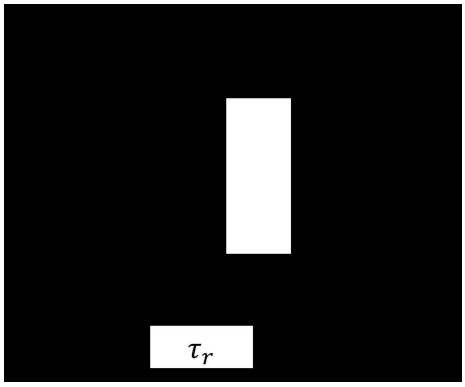

Figure 2.5: Relaxation Modulus. The relaxation modulus characterizes the viscoelastic materials stress relaxation over time.

Figure 2.5 illustrates that as time approaches infinity the modulus reaches a steady state. This region is known as "rubbery" response, which occurs above the materials glass transition temperature (T_g). During this phase, the material is more pliable (i.e., has a reduced stiffness) hence the term "rubbery." As an example the rubbery shear modulus is denoted by G_∞. The phase below T_g is known as the "glassy" response. The material has an increased stiffness during this phase. The instantaneous modulus, G_o, represents the maximum stiffness of the viscous (time-dependant) relaxation component [5]. The relaxation modulus can be defined by both the glassy and rubbery modulus. The mathematical form of the relaxation function is not

arbitrary; thermodynamic restrictions require it to be a monotonically decreascing function [4]. A linear viscoelastic relaxation function derived from the standard linear solid model can be expressed in the following equation [5]:

$$G(t) = G_\infty + G_o e^{\frac{-t}{\tau_r}} \tag{2.3}$$

where τ_r is the relaxation time, and t represents time. The instantaneous relaxation component corresponds to the time constant τ_r. The relaxation time is a time constant for the system to return to its steady-state, or rubbery region, in response to a disturbance where it is in its glassy region. The relaxation time is illustrated in Figure 2.5.

2.2.2 Dynamic Loading

Suppose that the stress $\sigma(t)$ from Eq. 2.2 varies sinusoidally with respect to time:

$$\sigma(t) = \sigma_o sin(2\nu t) \tag{2.4}$$

where ν represents the frequency. In linear viscoelastic materials subjected to harmonic oscillations, the strain is out of phase with the stress due to the internal material damping. This behavior corresponds to the viscous component of the material [2]. Figure 2.6 illustrates how the strain lags the stress for a viscoelastic material during cyclical loading.

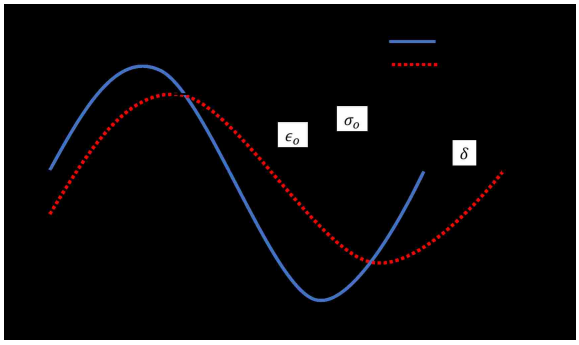

Figure 2.6: Cyclic behavior of viscoelastic material. The strain lags the stress by a phase shift.

The phase lag between the stress and strain can be represented by the phase angle, δ. The resulting out of phase strain is dependent on the phase angle and can be represented by:

$$\epsilon(t) = \epsilon_o sin(2\pi\nu t - \delta) \tag{2.5}$$

where ϵ_o is the instantaneous strain. As a result of the phase lag between stress and strain, a dynamic stiffness can be computed as a complex number E^* [4]:

$$\frac{\sigma}{\epsilon_o} = E^* = E' + iE'' \tag{2.6}$$

which the magnitude is:

$$|E^*| = \sqrt{(E')^2 + (E'')^2} \tag{2.7}$$

where single and double primes designate the real and imaginary parts; they do not represent derivatives; $i = \sqrt{-1}$. The E' in Eq. 2.7 represents the storage modulus, and E'' is the loss modulus. Both the storage and loss modulus can be related to the phase angle by the following:

$$E' = |E^*|cos(\delta) \tag{2.8}$$

$$E'' = |E^*|sin(\delta) \tag{2.9}$$

where the dynamic functions E',E'', and δ depend on frequency. The tangent of the loss angle is called the loss tangent ($tan(\delta)$) and is a measure of the internal damping [2]. The storage modulus E' is proportional to the energy stored within the material. The loss modulus E'' is proportional to the energy dissipated per cycle.

2.2.3 Constitutive Equations

Heretofore, all of the equations presented considered either transient or cyclical behavior; however, sometimes the loading history is arbitrary. Constitutive equations will be derived in order to predict the viscoelastic behavior with an arbitrary loading history. The Boltzmann superposition principle will be used to approximate the previous loading history into step functions. For this assumption, the strain history need not be a differentiable function of time [2]. Earlier, the instantaneous application of strain was represented by ϵ_o. Now, the instantaneous strain will be a applied with a Heaviside step function. This relation can be expressed in the following equation:

$$\epsilon(t) = \epsilon_o H(t) \tag{2.10}$$

where the Heaviside step function $H(t)$ is defined as:

$$H(t) = \begin{cases} 0 & t < 0 \\ \frac{1}{2} & t = 0 \\ 1 & t > 0 \end{cases} \tag{2.11}$$

A series of such step increases in strain can be used to describe any arbitrary strain input profile [2]. For an arbitrary strain history $\epsilon(t)$, consider a segment of time defined as $t - \tau$ where τ is a time variable. The τ in Eq. 2.12 should not be confused with the relaxation time in Eq. 2.4. A series of step increases in strain can be used to describe any arbitrary strain input profile. Therefore, for r discrete step increases

in strain, Eq. 2.10 can be recast as:

$$\epsilon(t) = \sum_{i=1}^{r} \Delta\epsilon_i H(t - \tau_i) \tag{2.12}$$

where the term $\Delta\epsilon_i$ represents the change in the strain magnitude for the i^{th} step occurring at time τ_i, and t is the current time [4].

Now, the Boltzmann superposition principle can be used to develop the constitutive equations for linear viscoelastic materials. The principle states that the effect of a compound cause is the sum of the effects of the individual causes [2]. Using Eq. 2.2, the resulting strain output can be determined with an arbitrary strain history using Eq. 2.12. The relaxation modulus is now taken over the time step and can be expressed as $E(\tau - t)$. Therefore, the resulting stress output can be expressed by:

$$\sigma(t) = \sum_{i=1}^{r} \Delta\epsilon_i E(t - \tau_i) H(t - \tau_i) \tag{2.13}$$

As the number of time steps increase to infinity Eq. 2.13 will eventually converge to a hereditary integral which leads to:

$$\sigma(t) = \int_0^t E(t - \tau) H(t - \tau) d\epsilon(\tau) \tag{2.14}$$

and τ is now a continuous time variable of integration representing the history effect. The Heaviside function in Eq. 2.14 will equal one since $\tau > 0$ is imposed and falls within the bounds of integration [2]. The constitutive relation for a linear viscoelastic material for a differentiable strain history can then be represented by the following:

$$\sigma(t) = \int_0^t E(t - \tau) \frac{d\epsilon(\tau)}{d\tau} d\tau \tag{2.15}$$

Consequently, the response of a linearly viscoelastic material to any load history can be found for the purpose of analysis or design [2]. For an instantaneous strain history expressed in Eq. 2.10, the transient stress response given by Eq. 2.2 can be

determined by Eq. 2.15. If there is a harmonic strain history $\epsilon(t)$ imposed, the stress in Eq. 2.15 can be represented by a complex number 2.9 [4]. Recall that the form of the shear relaxation function (Eq. 2.3) can also be used for the uniaxial relaxation modulus:

$$E(t) = E_\infty + E_o e^{-\frac{t}{\tau_r}} \tag{2.16}$$

If Eq. 2.16 is used as an input for 2.15, the complex moduli can be determined by the following set of equations [4].

$$E'(\omega) = E + E_o \frac{\omega^2 \tau_r^2}{1 + \omega^2 \tau_r^2} \tag{2.17}$$

$$E''(\omega) = E_o \frac{\omega \tau_r}{1 + \omega \tau_r} \tag{2.18}$$

where $\omega = 2\pi\nu$ (ν is the loading frequency).

2.3 Time-Temperature Superposition (TTS)

If an oscillatory strain is applied to a linear viscoelastic solid the oscillatory stress is:

$$\sigma(\omega) e^{-i\omega t} = E(\omega)\epsilon(\omega) e^{-i\omega t} \tag{2.19}$$

where $E(\omega)$ is a complex number that can be broken into Eq. 2.17 and Eq. 2.18. To determine the oscillatory relaxation modulus, $E(\omega)$, in a large frequency range, it is possible to measure $E(\omega)$ in a very limited frequency interval over a range of temperatures [6]. This procedure is known as Time-Temperature Superposition(TTS), and can be used with amorphous polymers. This procedure was first developed by Williams-Landel-Ferry(WLF) [7]. It states that the ratio of all mechanical relaxation times at temperature, T, to their values at a reference temperature, T_{ref}, can be expressed, after suitable choice of T_g, by the equation (WLF equation) [7]:

$$log(a_T) = -C_1 \left(\frac{T - T_{ref}}{C_2 + T - T_{ref}}\right) \tag{2.20}$$

where a_T is the shift factor that is dependent on temperature. Essentially, the frequency segments for each temperature are shifted along the frequency axis to obtain a continuous master curve. The master curve is a continuous curve that represents the relaxation behavior. The formulations presented in this section used the relaxation modulus, $E(\omega)$, that is usually determined in an oscillatory tensile test. However, TTS also holds for the shear relaxation modulus, $G(\omega)$, which is usually obtained in torsional experiments. In order to use TTS the material has to be a thermorheologically simple viscoelastic material. According to Ferry TTS holds when: (i) exact matching of shapes of adjacent (time or frequency dependent) curves is obtained; (ii) a_T has the same value for all viscoelastic functions; (iii) the temperature dependence of a_T has reasonable form (WLF, Arrhenius) [8]. The PDMS/PDPS copolymer was determined to be a thermorheologically simple material because TTS was used to construct the shear master curve presented in Section 3.1.1.

2.3.1 Prony Series

It is complicated to use viscoelastic materials in three-dimensional finite element analysis due to their time-dependent stress and strain profiles. In all FEA codes the stress tensor has to be computed and stored at each integration point and time step throughout the analysis. It can be computationally expensive to store the stress tensor at each integration point for viscoelastic materials because of their complex material properties. To simplify this process, a discrete series of exponentials called a Prony series is used to describe the relaxation modulus. The Prony series allows the current stress to be computed from a state variable stored from the preceding time step, thereby avoiding the need to store the stress at each time point in the analysis [9]. The relaxation modulus, $E(t)$, in Eq. 2.15 represents the material's time dependent relationship between stress and strain. There are a couple of restrictions placed on the relaxation modulus; specifically, it must be a continuous and monotonically

decreasing function to remain thermodynamically consistent.

For large problems, it is intractable to numerically solve Eq. 2.15. As a result, it is common to approximate the relaxation modulus, $E(t)$, using a discrete spectrum Prony series [9]:

$$E(t) = \sum_{i=1}^{N} E_i e^{-(\frac{t}{\tau_i})} + E_\infty \tag{2.21}$$

where E_i represents the Prony weight that is associated with the time constant τ_i. The Prony series is discrete because there is a finite number (N) of Prony terms. Both E_i and τ_i must be positive and satisfy the thermodynamic restrictions placed on $E(t)$.

2.4 SPEC model

Linear viscoelasticity theory can be used to develop material models. Most models use the application of TTS and Prony series. The viscoelastic model that was used for the PDMS/PDPS siloxane copolymer was the Simplified Potential Energy Clock (SPEC) model. The SPEC model is a thermodynamically consistent, phenomenological, fully nonlinear viscoelastic constitutive model. The model is based on the Potential Energy Clock (PEC) model [10]. These models have been used to successfully predict the viscoelastic behavior of glassy [11] and semi-crystalline [12] polymers. The model is built to capture the wide range of behavior observed in glassy polymers, including such phenomena as stress/volume relaxation.

The SPEC model uses a material clock that is driven by temperature, volume, and strain. The equations and parameters used to model the PDMS/PDPS will be outlined in this section. The equation that the SPEC model uses to calculate stresses

in glassy polymers is as follows:

$$\begin{aligned}\underline{\underline{\sigma}} = &\left[\Delta K \int_0^t ds f_v(t^* - s^*)\frac{dI_1}{ds}(s) - \Delta(K\beta)\int_0^t ds f_v(t^* - s^*)\frac{dT}{ds}(s)\right]\underline{\underline{I}} \\ &+ 2\Delta G \int_0^t ds f_s(t^* - s^*)\frac{d\underline{\underline{\epsilon_{dev}}}}{ds}(s) + [K_\infty I_1 - K_\infty \beta_\infty \Delta T]\,\underline{\underline{I}} + 2G_\infty \underline{\underline{\epsilon_{dev}}}\end{aligned} \tag{2.22}$$

where the subscript"∞" represents rubbery values. The terms ΔK and ΔG are the difference between the glassy and rubbery values. A full derivation and explanation of Eq. 2.22 can be found in the literature [11]. The material clock for Eq. 2.22 is:

$$t - s = \int_s^t \frac{dw}{a(w)} \tag{2.23}$$

where:

$$log(a) = -C_1\left(\frac{N}{C_2 + N}\right) \tag{2.24}$$

where a is the shift factor explained in section 2.3, and N is:

$$\begin{aligned}N = &\left[[T(t) - T_{ref}] - \int_0^t ds f_v(t^* - s^s)\frac{dT}{ds}(s)\right] \\ &+ C_3\left[I_1(t)_{ref} - \int_0^t ds f_v(t^* - s^*)\frac{dI_1}{ds}(s)\right] + C_4\left[\int_0^t ds f_s(t^* - s^*)\frac{\underline{\underline{\epsilon_{dev}}}(s)}{ds}\right]\end{aligned} \tag{2.25}$$

All but two of the parameters in Eq. 2.25, C_3 and C_4, are standard inputs to linear viscoelasticity [11]. For this analysis both C_3 and C_4 will be set to zero due to the linear viscoelasticity assumption.

Each of the parameters in Eq. 2.22 were determined to populate the SPEC model in Sierra/Solid Mechanics [13]. Table 2.1 gives a description of each of the parameters for the SPEC model.

Table 2.1: Parameters required by the SPEC equation

Symbol	Definition
T_{ref}	Reference temperature
K_∞	Rubbery bulk modulus
$\frac{dK_\infty}{dT}$	Derivative of K_∞ with respect to temperature
K_g	Glassy bulk modulus
$\frac{dK_g}{dT}$	Derivative of K_g with respect to temperature
β_∞	Rubbery coefficient of thermal expansion
$\frac{d\beta_\infty}{dT}$	Derivative of α_∞ with respect to Temperature
β_g	Glassy coefficient of thermal expansion
$\frac{d\beta_g}{dT}$	Derivative of α_g with respect to temperature
G_∞	Rubbery shear modulus
$\frac{dG_\infty}{dT}$	Derivative of G_∞ with respect to temperature
G_g	Glassy shear modulus
$\frac{dG_g}{dT}$	Derivative of G_g with respect to temperature
C_1	First Williams-Landel-Ferry (WLF) coefficient
C_2	Second WLF coefficient
f_v	Volumetric relaxation spectrum
f_s	Shear relaxation spectrum

Two relaxation functions are used to characterize the thermal and volumetric shear relaxation responses. Both the shear, f_s, and volumetric, f_v, relaxation spectrum's were determined. These functions are typically quite different and are expressed as a Prony series:

$$f_s(t) = \sum_{i=1}^{N} w_i e^{-\frac{t}{\tau_i}} \tag{2.26}$$

and:

$$f_v(t) = \sum_{j=1}^{M} w_j e^{-\frac{t}{\tau_j}} \tag{2.27}$$

where τ is the relaxation time, and w is the Prony weight. The Prony series used in Eq. 2.26 was used to fit the master curve that was explained earlier in section 2.3. To determine the volumetric spectrum for the PDMS/PDPS copolymer a single uniform-gradient (UG) finite element was used to predict the thermal strain data. The results for the volumetric relaxation function are provided in section 4.2.1.

An alternative method for representing the relaxation functions in SPEC is to use a streched exponential. The function takes the form of:

$$f(t) = exp\left(-\left(\frac{t}{\tau}\right)^{\beta}\right) \tag{2.28}$$

where the τ and β parameters can be varied until of the model matches the experimental data. Using the streched exponential will provide a new set of Prony terms and relaxation times.

Chapter 3

Experimentally Determining Viscoelastic Properties

3.1 Experiments

This chapter will present the experiments that were conducted to obtain the viscoelastic material properties of the PDMS/PDPS copolymer. The shear moduli and the two WLF coefficients were determined using commercial rheometers. There are multiple methods of determining the bulk modulus such as: pressure dilatometry, ultrasonic techniques, or measurements of Poisson's ratio in tension. Pressure dilatometry was chosen to determine the volumetric response of the PDMS/PDPS copolymer. The coefficient of thermal expansion (CTE) was obtained from commercial thermomechanical analyzers. Nearly all of the parameters for the SPEC model were extracted from the data. There where some assumptions that had to be made, and they are also presented in this chapter.

3.1.1 Experimentally Determining the Shear Coefficients

To determine the shear relaxation modulus of the material, a Dynamic Mechanical Analysis (DMA) was performed. The apparatus used was an ARES-G2 rheometer. Figure 3.1 displays the apparatus.

Figure 3.1: The shear response of the material of the material was calibrated using the ARES-G2 rheometer.

Both the glassy and long term shear moduli where determined. DMA measures the response of a material to a sinusoidal stress as described in Eq. 2.4. The basic principle of an oscillatory rheometer is to induce a sinusoidal shear deformation in the sample and measure the resultant shear stress response; the time scale probed is determined by the frequency of oscillation of the shear deformation.

For this experiment, the frequency ranged from 1 - 15 Hz. A forced convection oven was used to vary the temperature range from -100 °C to 50 °C. Due to the sample geometry, and the stiffness of the material, the experiment could not reach sub-ambient temperatures lower than -100 °C.

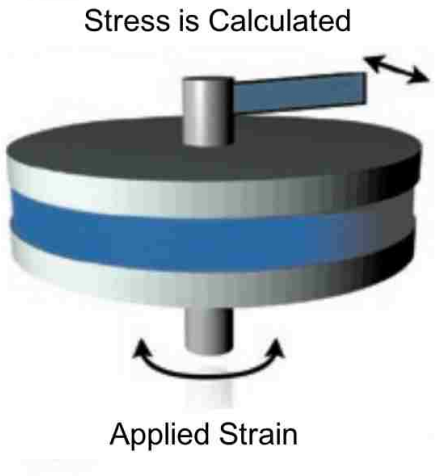

Figure 3.2: The experimental Rheology setup for DMA used to measure shear response (adapted from Weitz [1])

The test specimen was placed between two flat plates as seen in Figure 3.2 (adapted from Weitz) [1]. The plates are both 25 mm in diameter. A small normal force was applied to hold the apparatus together. The top plate remains stationary as a motor rotates the bottom plate, applying a time dependent strain. At the same time, the frequency dependent shear stress, $G(\omega)$, is calculated by measuring the torque that the sample imposes on the top plate [1]. The data from this experiment produced the storage modulus, loss modulus, $tan(\delta)$, and the oscillatory stress/strain. The data for this experiment is illustrated in Figures 3.3 - 3.5.

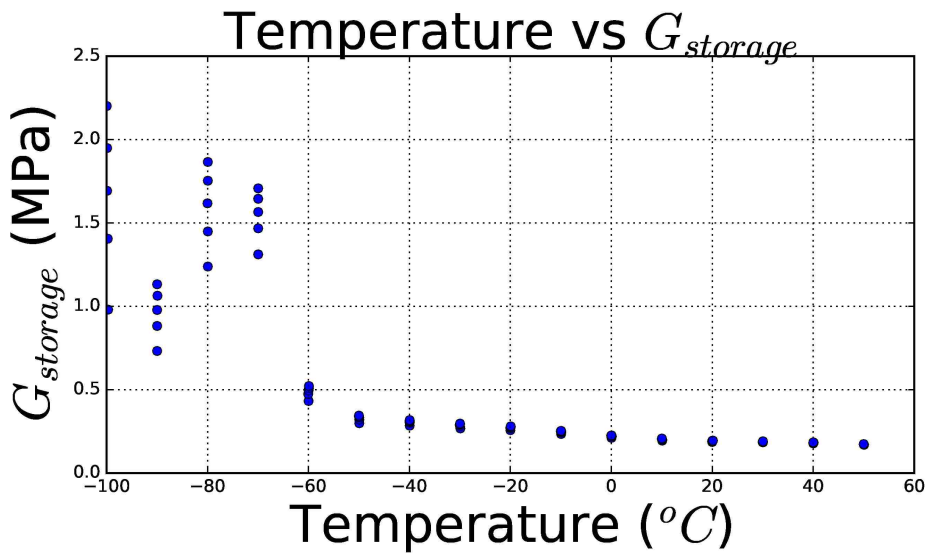

Figure 3.3: Experimental data for the storage modulus vs. temperature at multiple frequencies

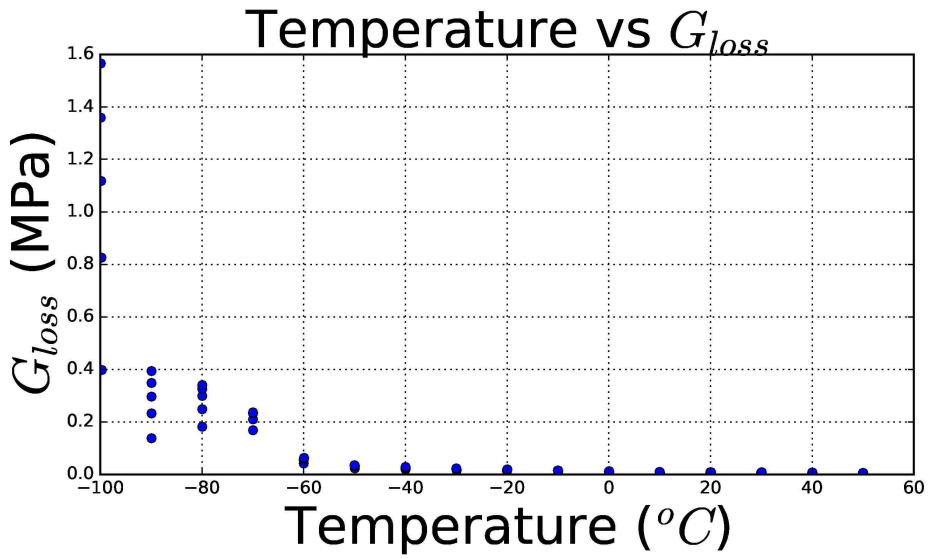

Figure 3.4: Experimental data for the loss modulus vs. temperature at multiple frequencies

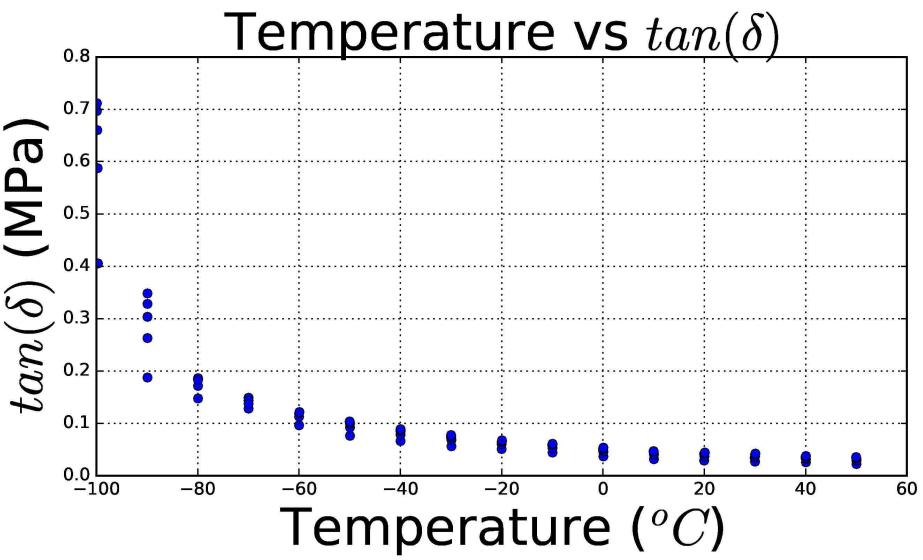

Figure 3.5: Experimental data for $tan(\delta)$ vs. temperature at multiple frequencies

Each data point represents a frequency of the storage modulus, loss modulus, and $tan(\delta)$. The data points at 15 Hz will be discarded because at higher frequencies inertial effects in the material start to become a concern. The DMA data presented in Figures 3.3-3.5 was calibrated in section 4.1.

3.1.2 Experimentally Determining Thermal Coefficients

A thermal mechanical analysis was used to determine the thermal properties of PDMS/PDPS. The apparatus used for this analysis was a PerkinElmer TMA 4000. Figure 3.6 displays the apparatus.

Figure 3.6: Apparatus used to determine thermal response of the material PerkinElmer TMA 4000.

The system has a linear variable differential transformer (LVDT) position sensor that provides sensitivity to small changes in volume and the ability to track large-dimensional changes. A small static force of 10 mN was applied to a test sample with a diameter of 3 mm and height of 8.814 mm. The experiment temperature started at -150 °C and was held constant for 20 minutes. The sample was heated from -150 °C to 70 °C with a heating rate of 2 °C per minute. Afterward, the sample was cooled back to the original temperature at the same rate it was heated. The thermal strain was calculated during the heating and cooling cycles. The experimental thermal strain data for this experiment can be seen in Figure 3.7.

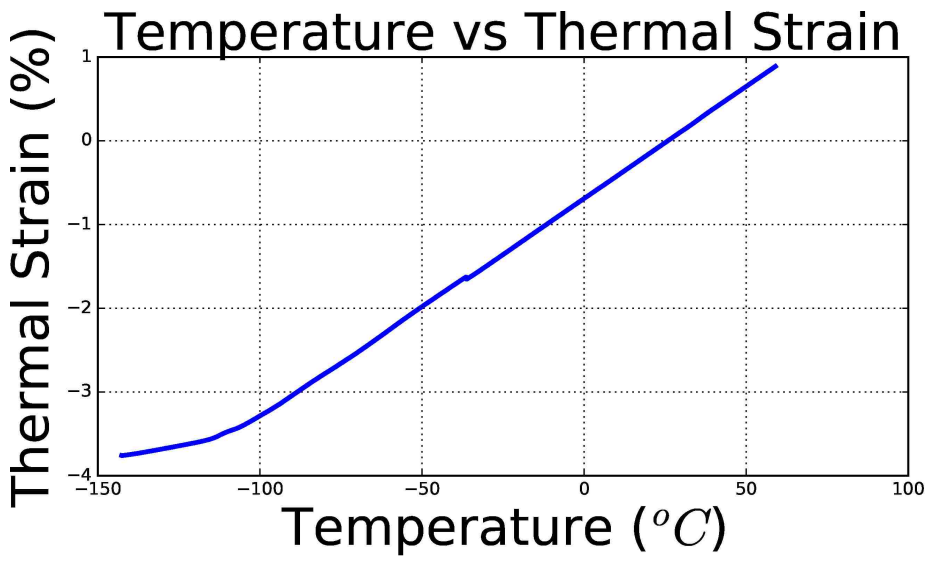

Figure 3.7: Experimental results for linear thermal strain of PDMS/PDPS.

According to the data in Figure 3.7 the T_g occurs in this material around -110^oC. The linear CTE for the material was determined by taking the derivative of the thermal strain data in Figure 3.7 as illustrated in Figure 3.8.

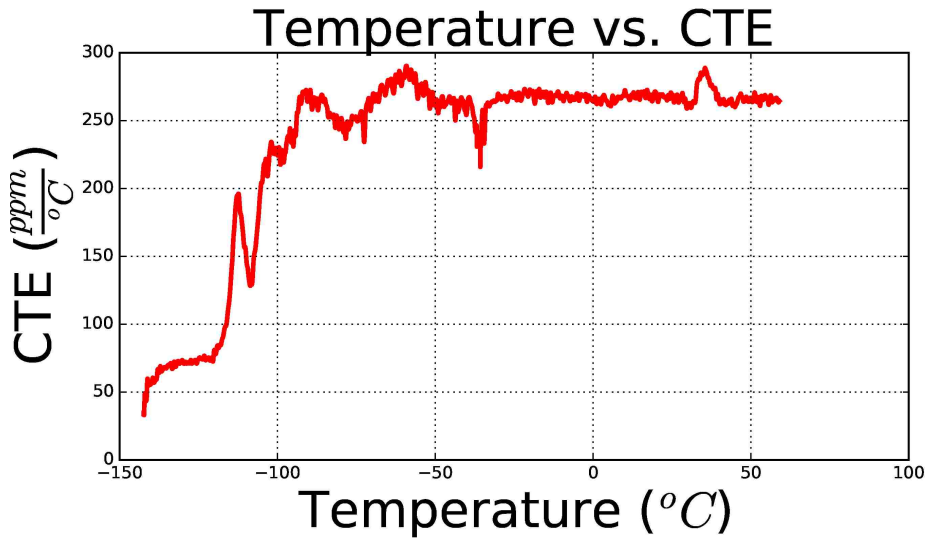

Figure 3.8: Experimental Thermal Strain

There was a small discrepancy in the thermal strain curve in Figure 3.7, that occurs around -40 °C. However, due to the size of this singularity it is negligible. The TMA data presented is analyzed in Section 4.2.

3.1.3 Experimentally Determining Bulk Modulus

Pressure dilatometry was used to determine the bulk modulus. The test sample was a cylinder 28.956 mm in height and a radius of 6.25 mm. Multiple LVDT's were placed strategically around the sample. The sample was placed inside a pressure vessel while being suspended in a hydraulic fluid. The LVDT's measured the volumetric changes as the hydrostatic pressure was increased. Figure 3.9 illustrates a plot of the experimental results.

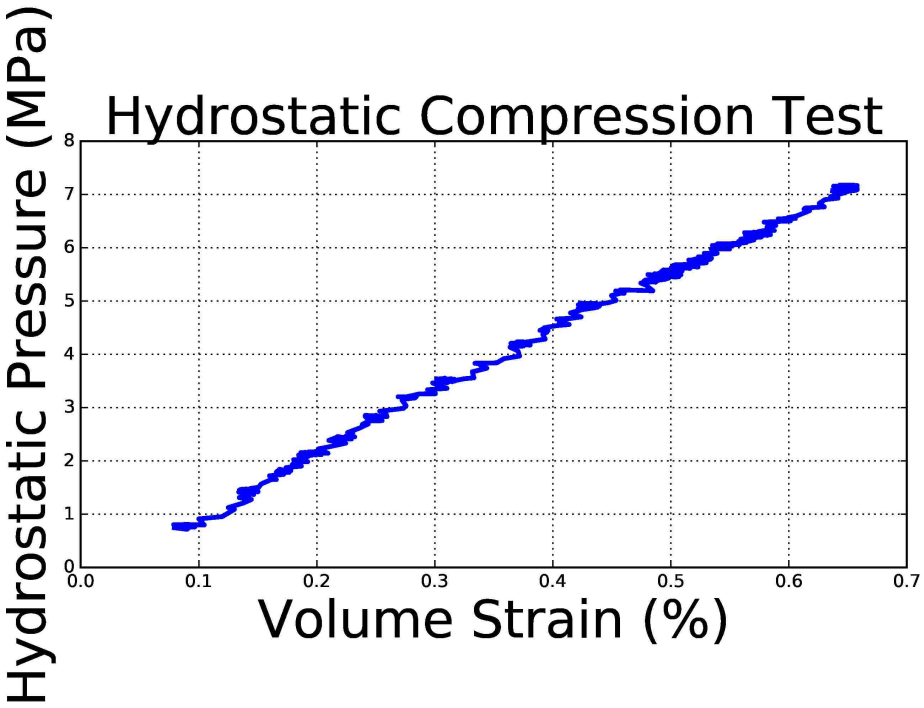

Figure 3.9: Hydrostatic response of the PDMS/PDPS copolymer.

This experiment was conducted at room temperature. Only the rubbery bulk modulus, K_∞, could be obtained from the experiment. It is often difficult to obtain data for the volumetric response at sub-ambient temperatures, due to crystallization occurring in the hydraulic fluid. The bulk response data presented in Figure 3.9 was analyzed and presented in section 4.3.

3.1.4 Experimentally Determining Flexural Storage Modulus

Another type of DMA performed was a three-point bend test. The data from this experiment will be used to calibrate the SPEC model. The apparatus used for this experiment was an RSA-G2 solids analyzer. Figure 3.10 displays the test set up for this procedure.

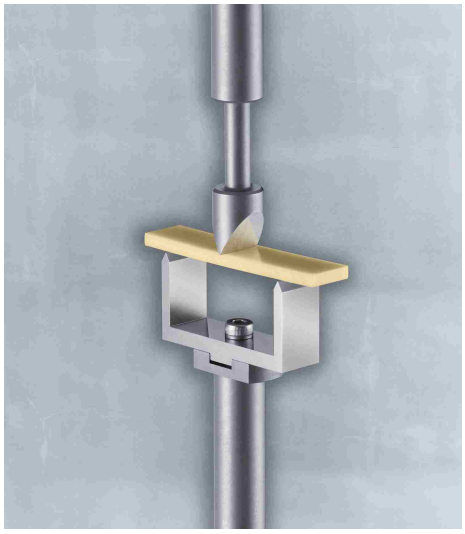

Figure 3.10: Three-point bend experimental setup on the RSA-G2 solids analyzer.

The sample is deformed around three point contacts at both ends and its middle. The geometry consisted of a rectangular square sheet 25 mm x 12.8 mm x 1mm.

The sample was subjected to a small oscillatory strain with a constant angular frequency of 1 Hz. The flexural modulus is computed by measuring the displacement of the material. The procedure starts at -140 °C, and is increased to 30 °C at a rate of 2 °C per minute. The data from this experiment is illustrated in Figure 3.11.

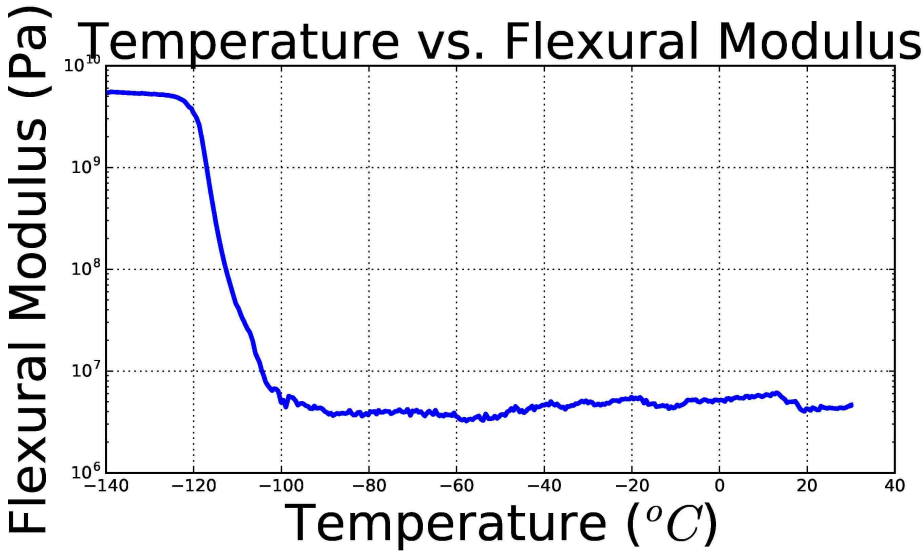

Figure 3.11: Experimental results for flexural storage modulus with three-point bend test.

The data in Figure 3.11 for the PDMS/PDPS copolymer is consistent with similar materials because there glassy and rubbery values are on the same magnitude and the overall shape is similar. However, above the glass transition temperature the data was pretty noisy due to very low forces.

3.1.5 Experimentally Determining Uniaxial Storage Modulus

An additional test was conducted to compare the uniaxial storage modulus to the flexural storage modulus that was determined in Section 3.1.4. The same RSA-G2 solid analyzer was used for this experiment. However, the experimental setup has changed. Figure 3.12 displays the configuration for this experiment.

Figure 3.12: Uniaxial experimental setup on the RSA-G2 solids analyzer.

The same frequency and temperature profile that was used for the three point bend test was used for this experiment. Ideally both the storage modulus and flexural modulus should have similar values. The data for the uniaxial test is provided in Figure 3.13.

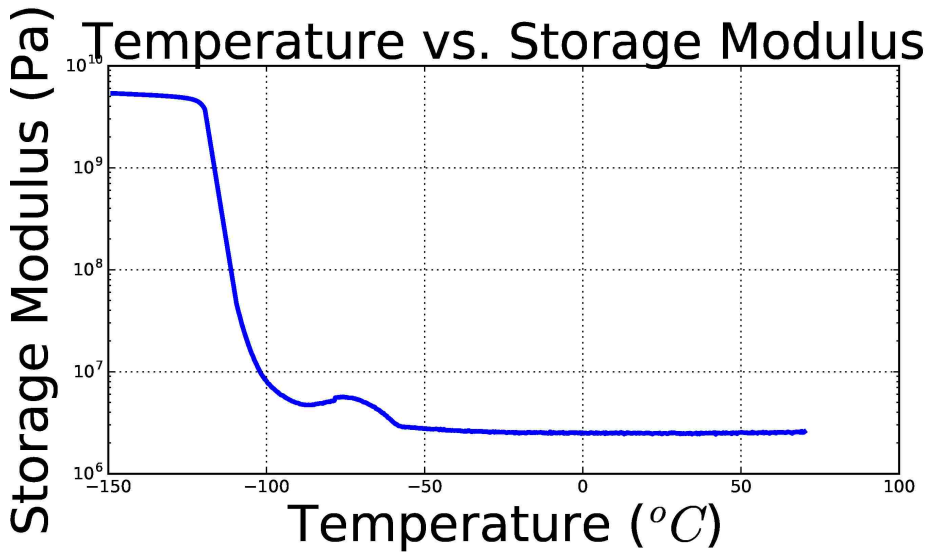

Figure 3.13: Experimental results for uniaxial storage modulus.

The uniaxial storage modulus matches up well with the flexural storage modulus from the three-point bend test. The glassy and rubbery values are similar in both experiments. The comparison between the uniaxial and flexural storage modulus is illustrated in Figure 3.14.

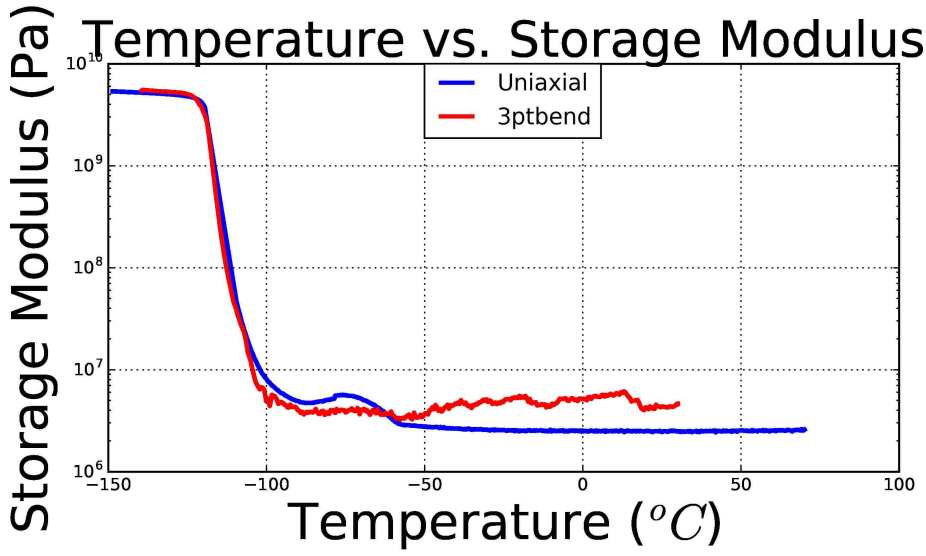

Figure 3.14: Comparison of experimental results for uniaxial and flexural storage modulus.

There is a sudden increase and then decrease in the uniaxial storage modulus data that occurs around -70^oC. It is unknown why this bump is occurring in the data. It could be due to experimental conditions, or the actual response of the material. One possibility is there could be crystallization occurring in the material. The overall shape of the uniaxial data is similar to that of the three-point bend. Therefore, because the data lines up well, and the origin of the bump is unknown, the uniaxial data can be used for calibration.

Chapter 4

Analysis of Experimental Results

4.1 Constructing the Shear Master Curve

This section will construct the shear master curve using the data presented in Section 3.1.1, and applying TTS described in Section 2.3. Recall that the relaxation modulus must be continuous and monotonically decreasing. The experimental data was smoothed after the frequency shifts were constructed in order to satisfy these conditions. The following figures show the logarithmic shifted frequency curves, and the smoothed curves. Both the storage modulus, $G_{storage}$, and the loss modulus, G_{loss}, as a function of shifted frequency are shown in Figure 4.1 and Figure 4.2, respectively.

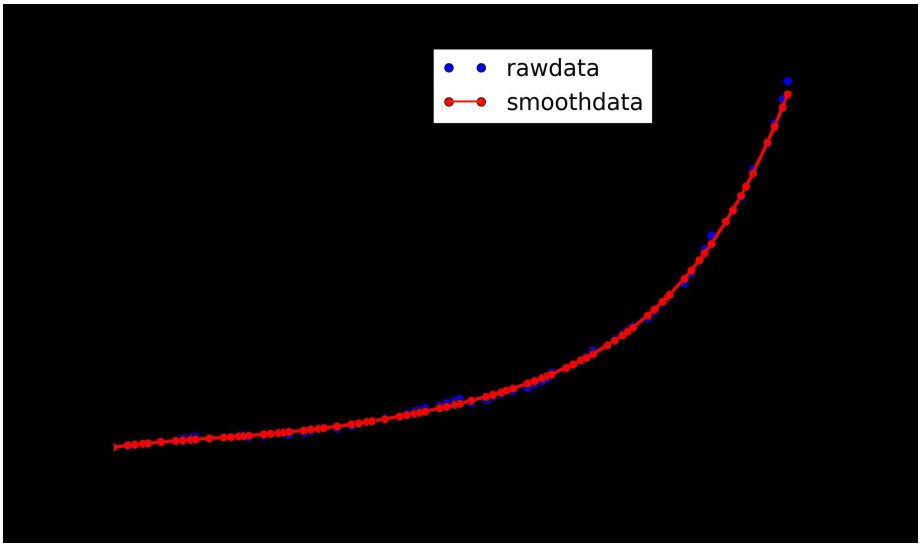

Figure 4.1: Smoothed and original data of the storage modulus after frequency shifts have been made.

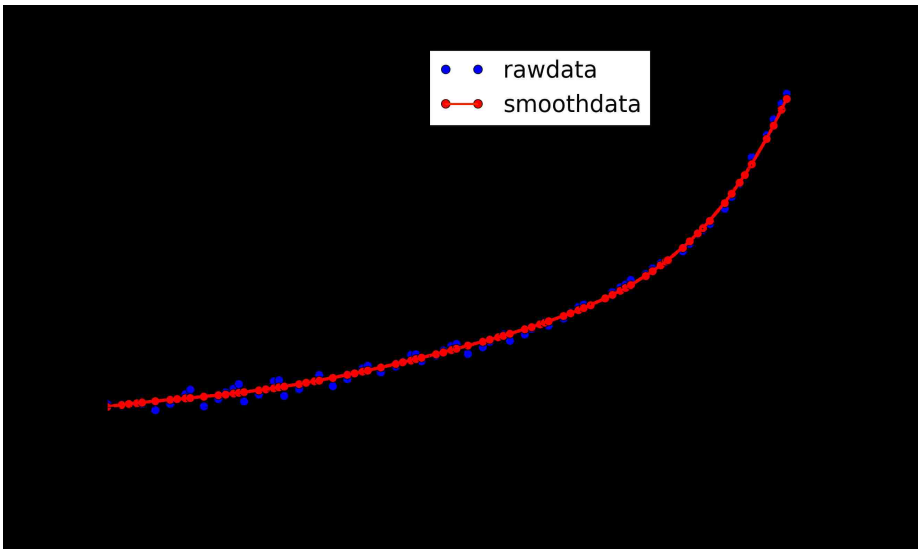

Figure 4.2: Smoothed and original data of the Loss modulus after frequency shifts have been made.

The new smoothed data creates a monotonically decreasing smooth curve. This will make it easier to fit a Prony series to the data. Figure 4.3 illustrates the logarithmic plot of $tan(\delta)$ vs. frequency.

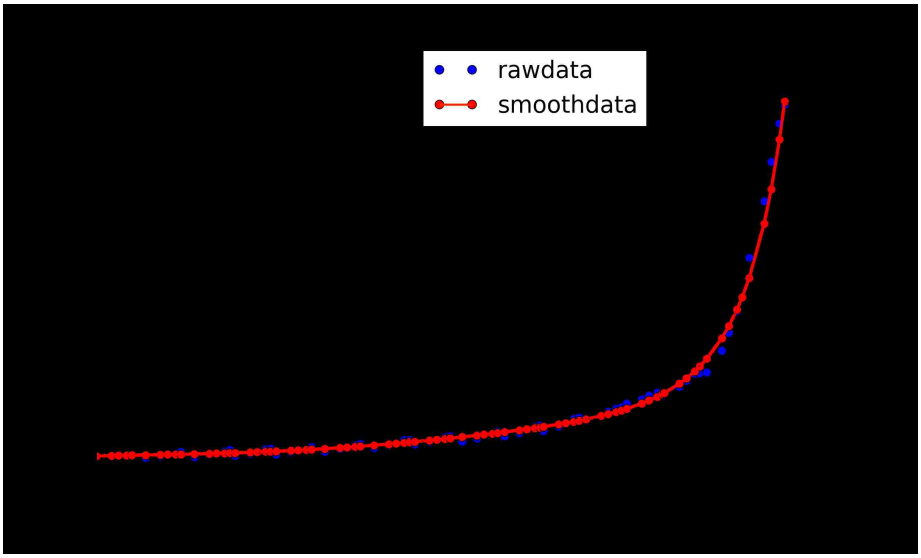

Figure 4.3: Smoothed and original data of $tan(\delta)$ after frequency shits have been made.

Section 2.3 also mentioned the WLF curve that is dependent on the shifted data. Figure 4.4 shows the WLF curve for the corresponding shifted data that was illustrated in Figures 4.1-4.3 as a function of temperature.

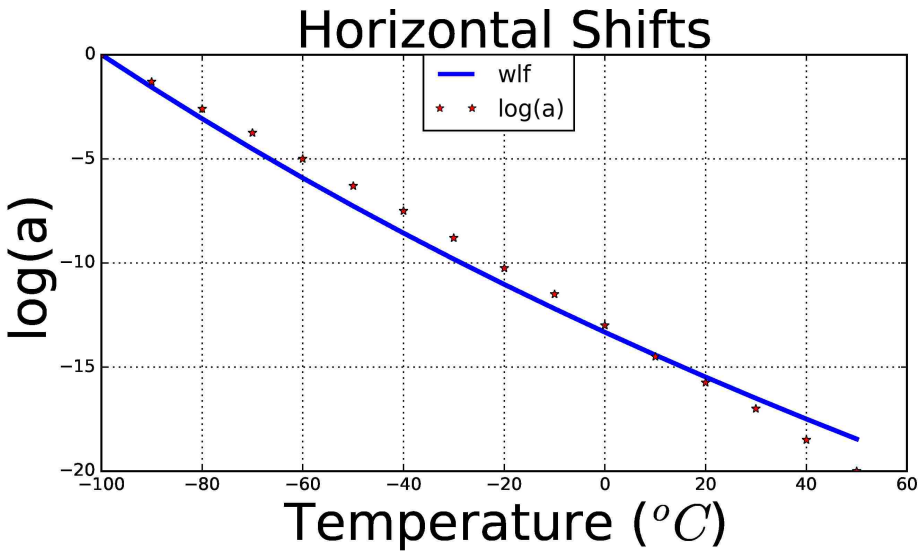

Figure 4.4: Log(a) as a function of Temperature, and the WLF fit.

The first WLF constant, C_1, has a dimensionless value of 80, and the second constant, C_2, has a value of 500 °C. One thing to note is the $log(a)$ values are high compared to other materials like Sylgard 184 [14].

4.1.1 Fitting Prony Coefficients to the Shear Master Curve

Now that the master curves have been constructed, the shear relaxation spectrum, f_s, mentioned in Section 2.4 can be determined. The Prony terms in Eq. 2.26 were fit to the data by defining a spectrum of relaxation times. The relaxation times started at the lowest frequency and incremented by decades to the largest frequency. An optimization study was conducted that discarded any negative Prony terms associated with the corresponding relaxation time. A total of 29 Prony terms were used. The values for the Prony terms and the corresponding relaxation times, τ_k, are listed in Appendix A. Figure 4.5 shows how well the Prony series approximates the master curve for the storage modulus constructed in section 4.1.

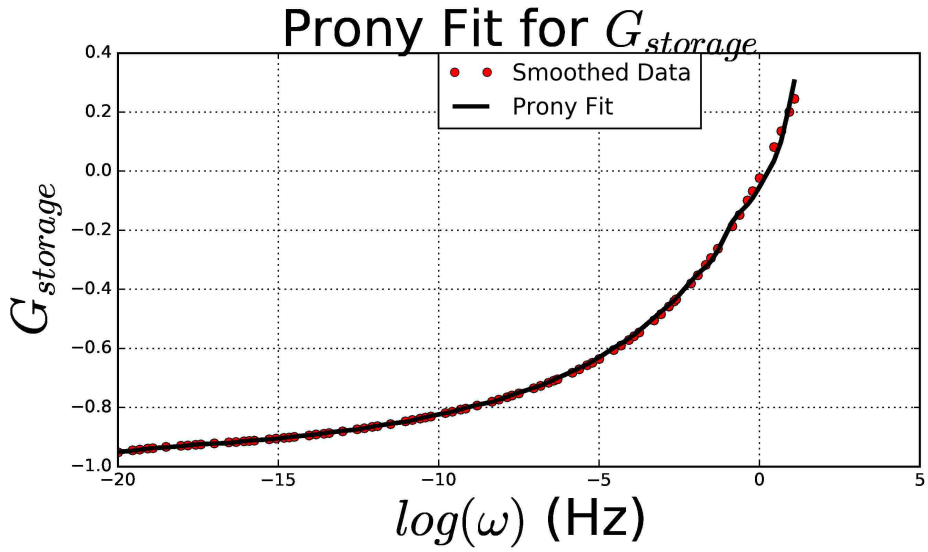

Figure 4.5: Prony series approximation for the storage modulus compared to the shifted and smoothed data.

It can be seen in Figure 4.5 that the Prony series matches up exceptionally well with the experimental data. The corresponding Prony fit for the loss modulus, G_l, is shown in Figure 4.6.

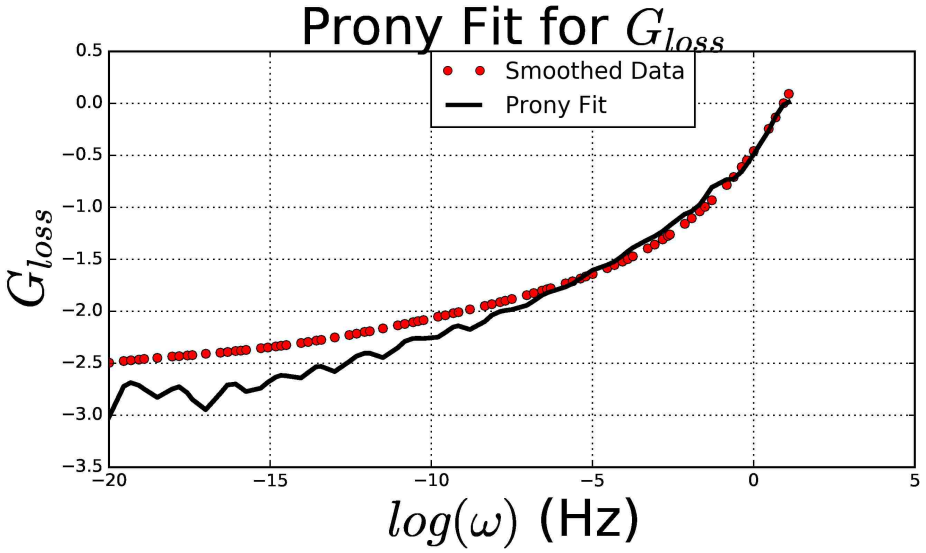

Figure 4.6: Prony series approximation for the loss modulus compared to the shifted and smoothed data.

The Prony series matches up well with the experimental data in the glassy region for the loss modulus illustrated in Figure 4.6. However, as the relaxation time increases the Prony series tends to deviate from the experimental data. Since in most applications of this material, the relaxation times are well below the point where the Prony series starts to deviate this is not a concern.

The Prony terms used to create the curves in Figures 4.5 - 4.6 can now be used in the SPEC model. In addition, the rubbery shear modulus and glassy shear modulus were determined by the fit. The glassy value for the PDMS/PDPS copolymer is 5.347 GPa, and the rubbery has a value of 2.576E-3 GPa.

4.2 Calibrating Thermal Expansion

The rubbery coefficient of thermal expansion (CTE), β_∞, and glassy CTE, β_g, were calibrated to the TMA data presented in section 3.1.2. The linear CTE, α, was determined in section 3.1.2, as illustrated in Figure 3.8. The volumetric CTE will have to be used in the SPEC model. For isotropic materials the volumetric thermal expansion coefficient is three times the linear coefficient. This ratio arises because volume is composed of three mutually orthogonal directions. Thus, in an isotropic material, for small differential changes, one-third of the volumetric expansion is in a single axis. The volumetric rubbery CTE, β_∞, is 8.07E-04 and the glassy CTE, β_g, is 2.1E-04 for the PDMS/PDPS copolymer.

4.2.1 Calibrating f_v using CTE Data

All of except for three parameters have been determined for the SPEC model. This only leaves the volumetric relaxation function $f_v(t)$. This parameter was defined by Eq. 2.27 in Section 2.4. To determine the volumetric spectrum a computational analysis was performed to predict the thermal strain response illustrated in Figure 3.8. The computational predictions were obtained using a single uniform-gradient (UG) finite element which was subjected to the same heating and cooling boundary conditions used in the TMA. The SPEC parameters determined in the previous section were used in Sierra/SM [13]. Figure 4.7 illustrates the comparison of the experimental and model data for the engineering strain vs. temperature.

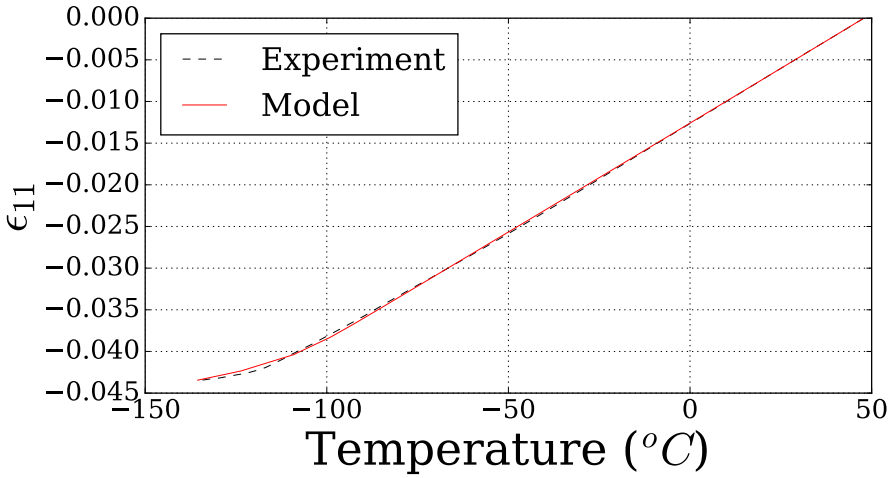

Figure 4.7: Computational prediction of thermal response compared to experimental data

Figure 4.7 shows how the SPEC model captures the change in thermal strain resulting from the glass transition. The model predictions match up well with the experimental data. The corresponding Prony values and relaxation times determined for the volumetric relaxation function, f_v, are listed in Appendix A.

4.3 Calibrating Experimental Bulk Data

Recall, in Section 3.1.3, the volumetric response of the material was determined by using pressure dilatometry. As mentioned before this experiment could only be conducted at room temperature. The rubbery bulk modulus was determined by taking the slope of the volumetric response illustrated in Figure 3.9. The SPEC model also requires an input for the glassy bulk modulus, K_g. For this parameter, previously published data for Sylgard 184 was used [14]. The value for the rubbery bulk modulus is 1.1 GPa and the glassy bulk modulus is 7.25 GPa for the PDMS/PDPS copolymer. It is extremely hard to measure bulk response at sub-ambient temperatures due to crystallization in the hydraulic fluid. Currently there is no solution for

obtaining these measurements. One possibility could possibly be using a gas instead of a liquid. This has not yet been tested, but might offer a solution.

The SPEC model was used to simulate the volumetric changes of the material with an applied hydrostatic pressure. For this a single uniform-gradient (UG) finite element with the same pressure boundary condition that was used in the simulation. Figure 4.8 shows the how the model predictions match up with the experimental data.

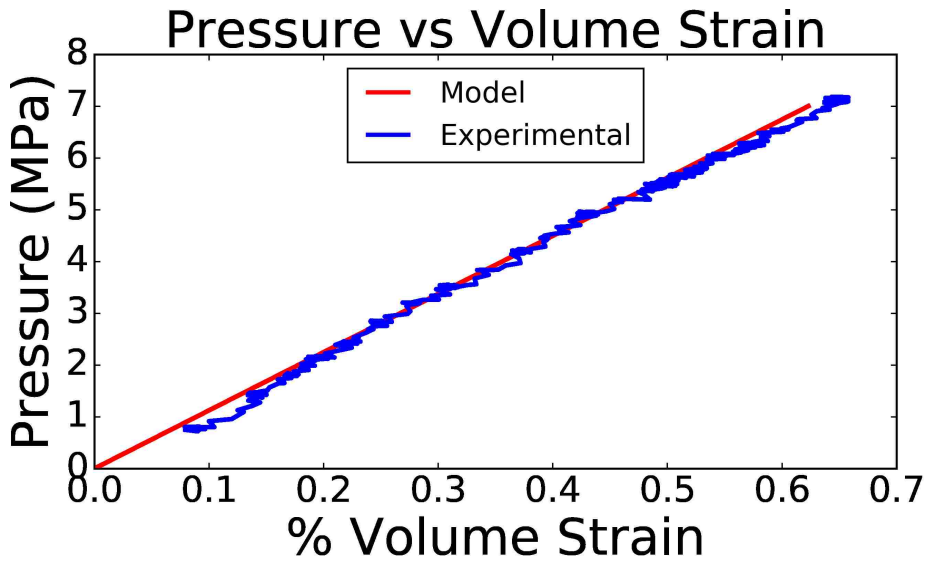

Figure 4.8: Comparison of model prediction for bulk modulus compared to experimental results.

The model predictions match up exceptionally well with the experimental data. This behavior was expected because the model inputs were directly taken from the experimental data. If data becomes available for the bulk response through T_g it would advised to conduct a simulation over the temperature range to see if the model accurately predicts the behavior.

4.4 Calibrating the Accuracy of the Viscoelastic SPEC Model

The calibrated SPEC parameters are listed in Table 4.1.

Table 4.1: Final Parameters for SPEC Model

Symbol	Definition	Units
T_{ref}	-100	^oC
K_∞	1.1	GPa
$\frac{dK_\infty}{dT}$	0	$\frac{GPa}{^oC}$
K_g	7.25	GPa
$\frac{dK_g}{dT}$	0	$\frac{GPa}{^oC}$
β_∞	8.07E-04	$\frac{ppm}{^oC}$
$\frac{d\alpha_\infty}{dT}$	0	-
β_g	2.100E-04	$\frac{ppm}{^oC}$
$\frac{d\alpha_g}{dT}$	0	-
G_∞	2.576E-3	GPa
$\frac{dG_\infty}{dT}$	0	$\frac{GPa}{^oC}$
G_g	5.347	GPa
$\frac{dG_g}{dT}$	0	$\frac{GPa}{^oC}$
C_1	80	-
C_2	500	^oC
f_s	See Appendix A	-
f_v	See Appendix A	-

In order to evaluate the accuracy of the populated SPEC model, the fitted parameters (Table 4.1) were used to predict the temperature-dependent uniaxial storage

modulus, E', that was experimentally determined in Section 3.1.5. An oscillatory uniaxial load was applied to a single UG finite element model with the same boundary conditions as the experiment. The comparison of the viscoelastic model predictions using the parameters listed in Table 4.1 to the experimental data for the storage modulus over multiple temperatures is illustrated in Figure 4.9.

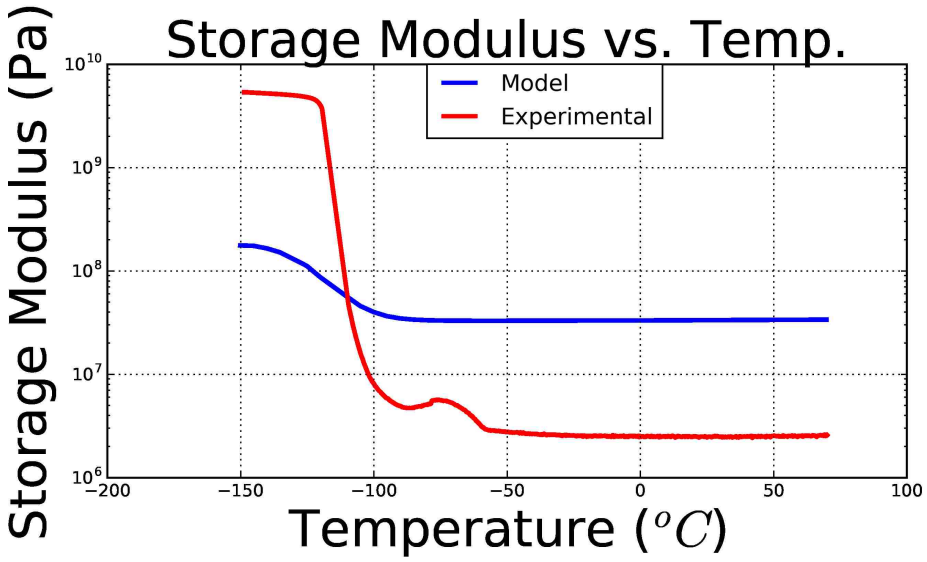

Figure 4.9: Model prediction of storage modulus at multiple temperatures.

The model under predicts the glassy region and over predicts the rubbery region. The glassy and rubbery shear values were measured experimentally and have some level of uncertaintyassociated with them. The uncertainty in these measurements could be the reason why the model is not predicting the experimental values. To acquire the correct shear modulus values the glass and rubbery shear modulus was varied until the model accurately predicts the two regions. The new comparison with the calibrated shear values are illustrated in Figure 4.10.

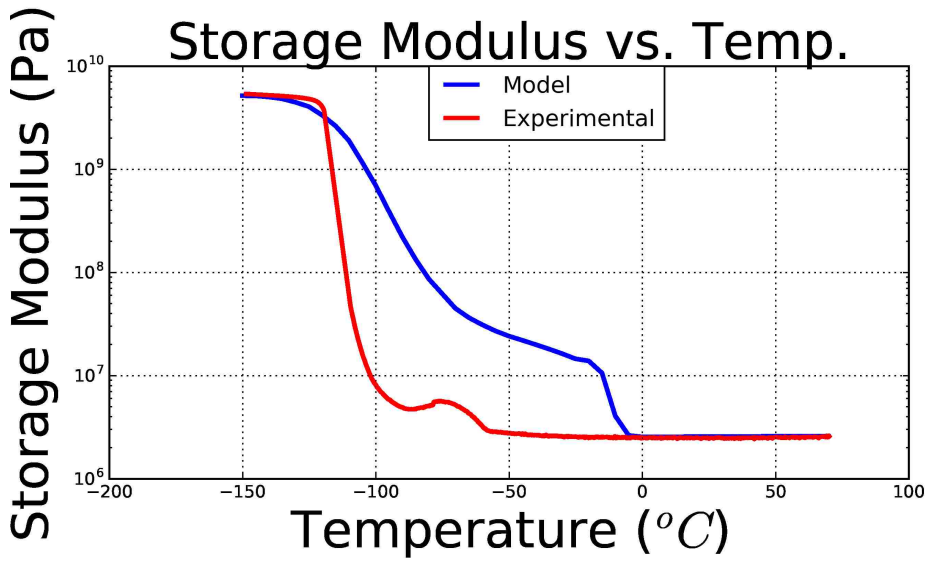

Figure 4.10: Model prediction of storage modulus at multiple temperatures with calibrated shear values.

The predictions match up well with the glassy and rubbery region of the experimental data. However, the glass transition temperature of the model does not match that of the experiment. In Section 2.4, a new method was introduced that used a stretched exponential to represent the shear relaxation function in the SPEC model. This new approach will provide a new set of Prony terms and relaxation times. Figure 4.11 illustrates the relaxation function vs. time when using the stretched exponential.

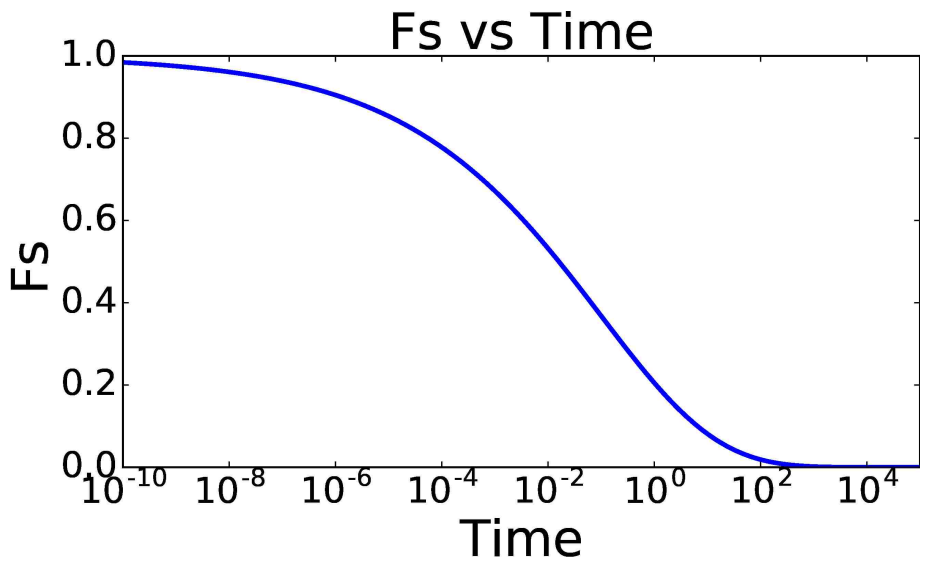

Figure 4.11: Shear relaxation function using a stretched exponential using calibrated τ_s and β_s values.

The new model comparison using the stretched exponential is illustrated in Figure 4.12.

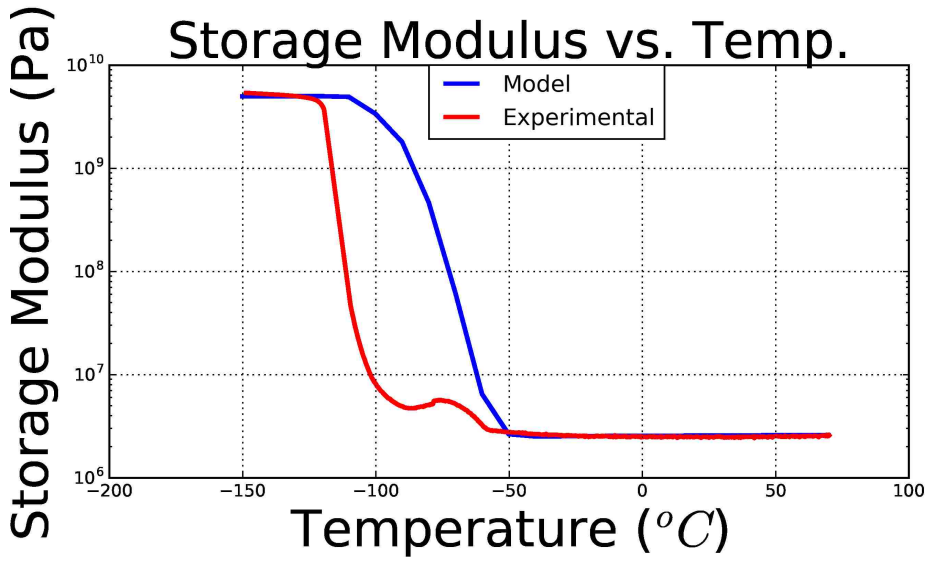

Figure 4.12: Model prediction of storage modulus at multiple temperatures using stretched exponential.

The glass transition does still occur at a slightly higher temperature than the experimental data, but it is a better prediction than using the original values that were used in Figure 4.9. The SPEC parameters used for the model predictions in 4.12 are listed in Table 4.2.

Table 4.2: Final Parameters for SPEC Model

Symbol	Definition	Units
T_{ref}	-100	^oC
K_∞	1.1	GPa
$\frac{dK_\infty}{dT}$	0	$\frac{GPa}{^oC}$
K_g	7.25	GPa
$\frac{dK_g}{dT}$	0	$\frac{GPa}{^oC}$
β_∞	8.07E-04	$\frac{ppm}{^oC}$
$\frac{d\alpha_\infty}{dT}$	0	-
β_g	2.100E-04	$\frac{ppm}{^oC}$
$\frac{d\alpha_g}{dT}$	0	-
G_∞	2.576E-3	GPa
$\frac{dG_\infty}{dT}$	0	$\frac{GPa}{^oC}$
G_g	26.735	GPa
$\frac{dG_g}{dT}$	0	$\frac{GPa}{^oC}$
C_1	80	-
C_2	500	^oC
τ_s	1.0E-5	s^{-1}
β_s	0.1	-
τ_v	6.0	s^{-1}
β_v	0.14	-

4.5 Applications of the SPEC model

The overall goal of this research was to accurately predict the viscoelastic behavior of the PDMS/PDPS copolymer in preload conditions followed by a consistant held load, and also in shock environments. To see how the SPEC model captures the viscoelastic response of the material during preload environments a single finite element was used in Sierra/SM to simulate loading conditions. A force of 200 N was applied to one side of the element in one direction while the opposing side was held fixed. The force gradually increased with a cosine ramp function illustrated in Figure 4.13.

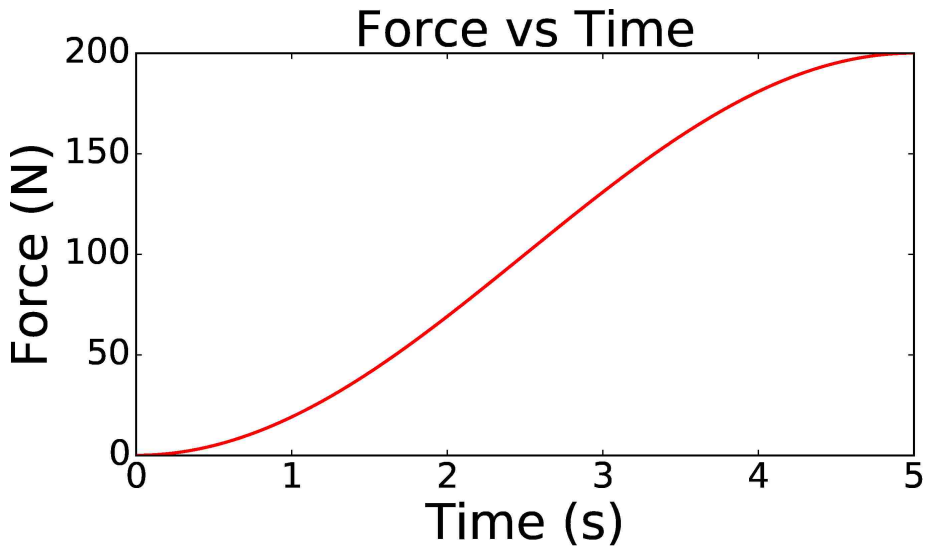

Figure 4.13: Smooth loading boundary condition for preloading single finite element.

The displacement was measured at the nodes that the force in Figure 4.13 was applied. Figure 4.14 illustrates how the displacement changes with time as the 200 N force is being applied.

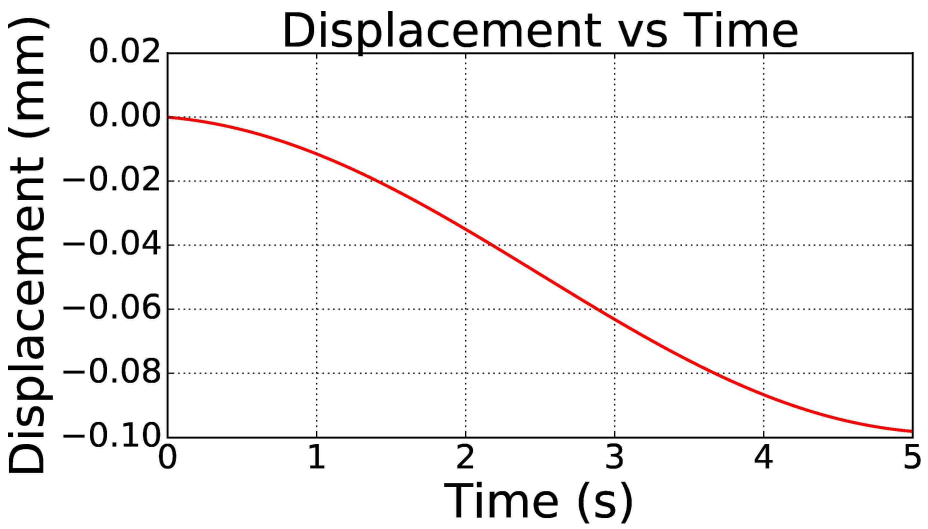

Figure 4.14: Displacement vs. Time with a 200 N force applied.

As the force is being applied the displacement decreases until it reaches the end of the force ramp. To see if the SPEC model captures any of the viscoelastic behavior such as creep and stress relaxation the force is held constant after it reaches its maximum value of 200 N. Figure 4.15 illustrates the displacement of the material during the consistant loading conditions for one hour.

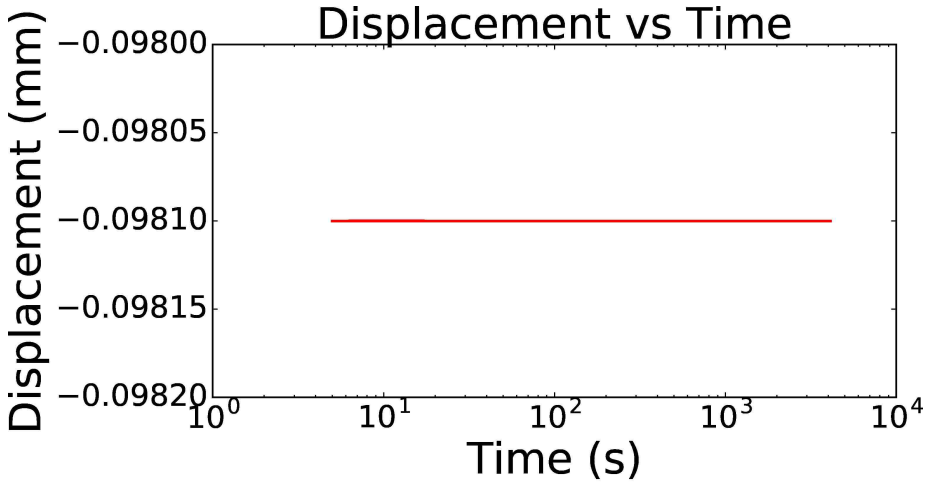

Figure 4.15: Relaxation occurring in model with constant force held for over an hour.

Most preload cases are held for longer than an hour, but Figure 4.15 shows that there is not a significant change in displacement for long periods of time. This is because the creep that occurs in the material happens quickly. Figure 4.16 shows the displacement response in the first minute of the constant force. The displacement is significantly smaller, so the displacement axis was normalized to better illustrate the viscoelastic behavior occurring.

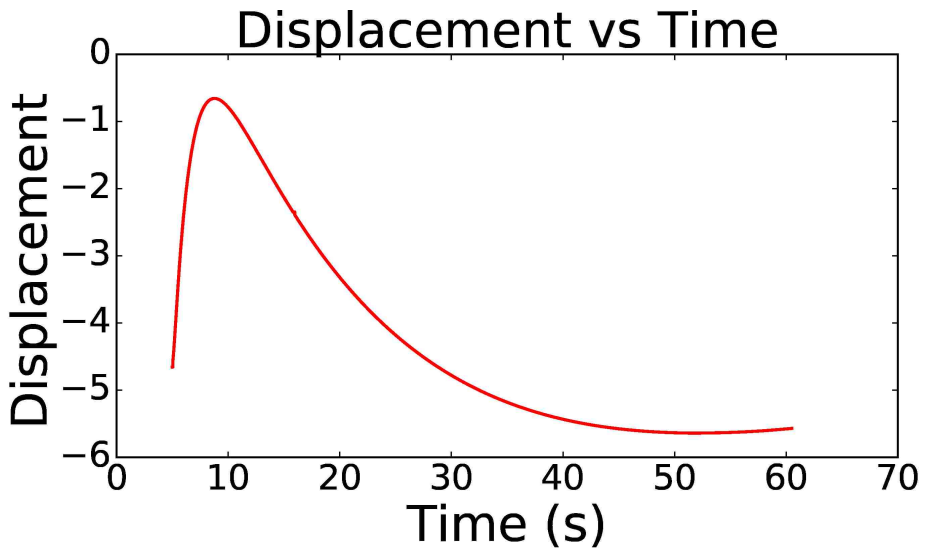

Figure 4.16: Relaxation occurring in model with constant force held for one minute.

The SPEC model captures the creep that occurs in the material during the first 20 seconds while the preload is held constant. Then the displacement starts to increase again until it reaches equilibrium where it is at a constant displacement for the rest of the simulation. Even though the displacements are small during the period of time when the force is held constant, they are important to be aware of.

The PDMS/PDPS copolymer is also used in applications such as tires or aircraft. These applications subject the material to multiple shock environments. To simulate these environments a single finite element was subjected to an applied acceleration in one direction. The arbitrary shock used for the simulation is illustrated in Figure

4.17.

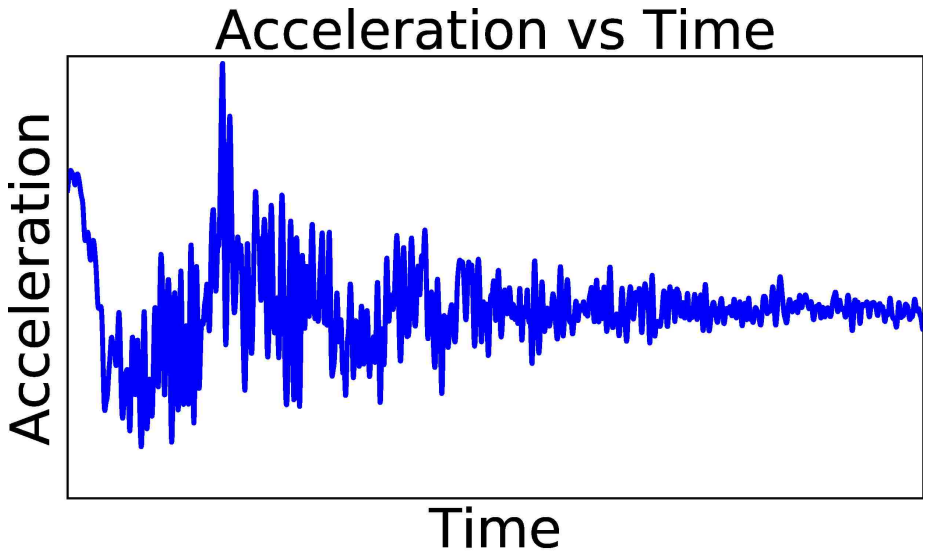

Figure 4.17: Applied shock environment.

To show the difference between the calibrated SPEC model and other models the von Mises stress was compared to a Mooney Rivlin model for a similar material. Figure 4.18 illustrates the von Mises stress of the material during the shock environment.

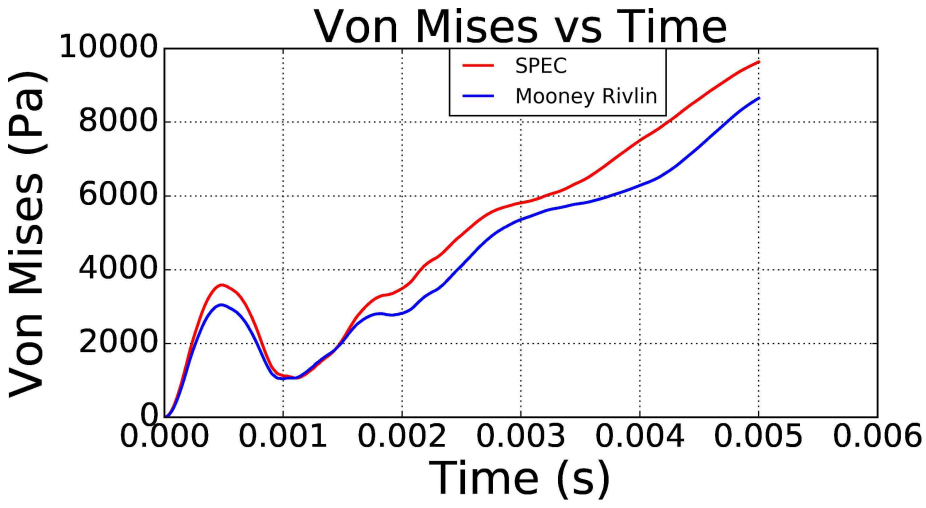

Figure 4.18: von Mises stress vs. time for the applied shock boundary condition.

The overall shape between the two models during the shock simulation are similar. However, the stress values are different between them. As time continues to increase during the simulation the larger the difference in the stress values between the models. The SPEC model captures a larger stress state than the Mooney Rivlin model.

Chapter 5

Conclusions

The work presented in this report is a summary of the calibration for PDMS/PDPS copolymer using various experimental procedures and the viscoelastic SPEC model. The viscoelastic behavior for the PDMS/PDPS copolymer have yet to be determined until now. The shear moduli were determined by using DMA testing. The data obtained from the DMA was used to create a shear master curve for the material using the application of TTS and fitting a Prony series to the master curve. Once the shear master curve was constructed both the rubbery and glassy shear moduli were determined as well as the WLF coefficients. It was determined that the relaxation function did not accurately predict the glass transition when the model was compared to experimental uniaxial data. A stretched exponential was used to create new Prony terms and relaxation times to calibrate the model to uniaxial storage modulus data. The rubbery bulk modulus was determined by the pressure dilitometer. The glassy bulk modulus was assumed to be similar to Sylgard 184. The rubbery and glassy CTE values were determined by TMA. The TMA data was also used to determine the volumetric relaxation function.

The populated SPEC model can now be used to simulate multiple applications for

which the silicone rubber may be used. It was shown that the model can be used for predicting both shock and preloading applications. The viscoelastic behavior of the material was captured in the preload case using the SPEC model. Also, it was shown that the SPEC model captures a different stress state when compared to other models during shock environments.

5.1 Future Work

One of the short comings of the model is that the glassy bulk modulus, K_g, was not obtained through experimentation. As it stands, most pressure dilatometers do not have the capability to reach sub-ambient temperatures. Coming up with an experimental procedure to measure the bulk modulus at colder temperatures would be highly beneficial. It would help improve the accuracy of the model, and allow for better understanding of this parameter. Also, it could be used for another validation technique for predicting volumetric response throughout the materials temperature dependent range.

As mentioned in section 3.1.1, the DMA was not able to reach sub-ambient temperatures lower than -100 °C. If measurements below the T_g could be obtained it would allow the model to be used in a wider range of applications. It would be possible to obtain this data if different sample geometry was available.

Appendix A

Prony Terms and Relaxation Times

Table A.1: Prony terms for the shear relaxation function

Prony Term	relaxation time
6.90545929e-01	8.20571980e-02
9.38524924e-02	9.89564331e-01
9.28911314e-02	1.19335974e+01
3.20773206e-02	1.43912571e+02
1.17727261e-02	4.99761052e+02
1.32204749e-02	1.73550585e+03
1.23357611e-02	6.02684131e+03
4.91126605e-03	2.09292387e+04
8.99414879e-03	7.26803661e+04
4.48650599e-03	2.52395020e+05
3.96960692e-03	8.76484934e+05
4.92863883e-03	3.04374406e+06
2.10156570e-03	1.05699226e+07
2.78459077e-03	3.67058664e+07
3.57275204e-03	1.27467408e+08
3.45560815e-03	1.53718630e+09
7.20338172e-04	5.33814270e+09
1.52516596e-03	1.85376148e+10
2.11960521e-03	6.43750425e+10
1.55031123e-03	7.76327335e+11
1.19037131e-03	2.69592964e+12
1.55092161e-03	3.25114173e+13
1.03674180e-03	3.92069675e+14
5.44479491e-04	1.36152910e+15
1.18409771e-03	1.64192863e+16
6.26831620e-05	1.98007493e+17
1.06834569e-03	6.87614935e+17
4.87279837e-04	8.29225503e+18
1.05913974e-03	2.87962759e+19

Table A.2: Prony terms for the volumetric relaxation function

Prony Term	relaxation time
6.25672474e-02	1.23607138e-06
2.23797281e-03	5.32346686e-06
4.58570909e-02	2.29269117e-05
4.45947999e-02	9.87407820e-05
7.45425573e-02	4.25253176e-04
9.66983627e-02	1.83146477e-03
1.28953881e-01	7.88768527e-03
1.53801560e-01	3.39703934e-02
1.60796015e-01	1.46302444e-01
1.34305718e-01	6.30089996e-01
7.21520950e-02	2.71364847e+00
2.34927008e-02	1.16870416e+01

Bibliography

[1] P. H. W. D. Weitz, David and R. Larsen., "Measuring the viscoelastic behaviour of soft materials," vol. n., Apr. 2007.

[2] R. S. Lakes, *Viscoelastic Materials.* New York: Cambridge: Cambridge, 2014.

[3] H. Markovitz, "Boltzmann and the beginnings of linear viscoelasticity," vol. 1, Apr. 1977.

[4] K. L. Troyer, *Viscoelastic Characterization and Modeling of Musculoskeletal Soft Tissues.* Doctoral dissertation, Colorado State University, Colorado, USA, Apr. 2012.

[5] J. Vincent, *Structural Biomaterials.* New Jersey: Princeton: Princeton University Press., 2012.

[6] W. P.-H. Lorenz, B. and B. Persson., "The temperature dependence of relaxation mechanisms in amorphous polymers and other glass-forming liquids," vol. Polymer, Apr. 1955.

[7] O. D. MALCOLLM.WILLIAMSR, "Master curve of viscoelastic solid: Using causality to determine the optimal shifting procedure, and to test the accuracy of measured data.," vol. Polymer, Apr. 2014.

[8] J. Ferry, *Viscoelastic Properties of Polymers.* New York: Willey, 1980.

[9] S. Park and R. Schapery., "Methods of interconversion between linear viscoelastic material functions. part i a numerical method based on prony series.," vol. 36, Apr. 1999.

[10] D. B. A. R. S. C. Caruthers, James M. and P. Shrikhande., "A thermodynamically consistent, nonlinear viscoelastic approach for modeling glassy polymers.," vol. Polymer, Apr. 2004.

[11] R. S. C. Adolf, Douglas B. and M. A. Neidigk., "A simplified potential energy clock model for glassy polymers.," vol. Polymer, Apr. 2009.

[12] D. Adolf, "Modeling the response of monofilament nylon cords with the nonlinear viscoelastic, simplified potential energy clock model.," vol. Polymer, Apr. 2010.

[13] S. S. M. Team, *Sierra/SolidMechanics 4.44 User's Guide.* Box 5800 Albuquerque, NM 87185-0380: Sandia National Laboratories, 2016.

[14] B. J. Long Kevin, "A linear viscoelastic model calibration of sylgard 184," Sandia Report SAND2017-4555, Sandia National Laboratories, P.O. Box 5800, Albuquerque, NM., 87185, Apr. 2017.